sciendo

CIVIL AND ENVIRONMENTAL ENGINEERING REPORTS

E-ISSN 2450-8594

CEER 2021; 31 (4): 0148-0166
DOI: 10.2478/ceer-2021-0054
Original Research Article

THE APPLICATION OF SENTINEL-2 DATA FOR AUTOMATIC FOREST COVER CHANGES ASSESSMENT – BIAŁOWIEŻA PRIMEVAL FOREST CASE STUDY

Renata PELC-MIECZKOWSKA[1]
University of Warmia and Mazury in Olsztyn, Faculty of Geoengineering

A b s t r a c t

Sentinel-2 mission, as a part of European Space Agency Earth Observation Program Copernicus, designed specifically for Earth surface observations provides images in 13 bands. That imaging is used to analyse many subject areas as Land monitoring, Emergency management, Security and Climate change. In the presented paper the application of Sentinel-2 data for automatic forest cover changes detection has been analysed. As input data, B02, B03, B04 and B08 bands have been used to compute Normalized Difference Vegetation Index (NDVI) and Enhanced Normalized Difference Vegetation Index (ENDVI). To track changes in the forest cover over the years, for each pixel the difference in the value of vegetation indices between consecutive years have been calculated. Then the threshold was set at the level of 0.15. The values of differences above the threshold mean a significant decrease in the quality of vegetation and may be considered areas of deforestation.

Keywords: remote sensing, radiometric indices, Sentinel-2, forest cover

1. INTRODUCTION

Sentinel-2 is a satellite mission launched as part of the Earth Operation (EO) program by the European Space Agency [1]. As part of this program, two twin-

[1] Corresponding author: University of Warmia and Mazury in Olsztyn, Faculty of Geoengineering, Heweliusza 12, 10-724 Olsztyn, Poland, e-mail: renata.pelc@uwm.edu.pl

satellites were launched that perform imaging with high resolution and high revisit frequency (5 days at the equator). Satellites (SENTINEL-2A and SENTINEL-2B) operate simultaneously on the same orbit phased at 180° at a mean altitude of 786 km. To ensure high quality of the position of the satellites, they are positioned using dual-frequency GNSS receivers. Each satellite is equipped with a MultiSpectral Instrument (MSI) with a Field of View (FoV) of 290 km [2]. MSI works passively so it receives sunlight reflected from the Earth's surface. Inside the MSI, the light beam is split into two separate focal planes by a filter. One of the focal planes is responsible for the Visible and Near-Infra-Red (VNIR) bands and the other one for the Short Wave Infra-Red (SWIR) bands. In total, as a result of the operation of satellites, 13 bands are recorded. Four visible and near-infrared bands with 10m spatial resolution, six red edge and shortwave infrared bands with 20 m spatial resolution and three atmospheric correction bands with 60 m spatial resolution (Table 1) [3].

Table 1. The spectra bands and their resolution for Sentinel-2 MultiSpectral Instrument

BAND NAME	SPECTRAL REGION	CENTRAL WAVELENGTH (MM)	RESOLUTION (M)
B1	Coastal aerosol	0.443	60
B2	Blue	0.490	10
B3	Green	0.560	10
B4	Red	0.665	10
B5	Vegetation Red-edge 1	0.705	20
B6	Vegetation Red-edge 2	0.740	20
B7	Vegetation Red-edge	0..783	20
B8	NIR (Near-InfraRed)	0.842	10
B8A	NIRn (Near-InfraRed narrow)	0.865	20
B9	Water vapour	0.945	60
B10	SWIR - Cirrus (Shortwave infrared)	1.375	60
B11	SWIR 1	1.610	20
B12	SWIR 2	2.190	20

Sentinel-2 imaging is used to analyze many subject areas. They mainly include: Land monitoring, Emergency management, Security and Climate change [4-7]. It is a tool that is used commonly to analyze changes in land use and to analyze areas of drought [8-11]. Imaging is also very popular in the analysis of green vegetation due to the spectral response of chlorophyll [12-14]. Healthy vegetation, thanks to the high content of chlorophyll, strongly absorbs the blue band (0.490 μm) and

the red band (0.665 μm) and reflects the green band (0.560 μm). At the same time, healthy vegetation strongly reflects the NIR bands (0.842 μm) [15]. The way of absorption and reflection of individual bands differs depending on the vegetation, therefore multispectral analyzes can be used to determine the types of vegetation that cover a given area. At the same time, many analyzes are performed to determine changes in the afforestation area or the state of the tree cover [18-22].

In recent years, there have been changes in forest management in Poland. These changes also concerned the Białowieża forest which is one of the largest primeval forest landscapes in Europe. As a result of these changes, there was a significant felling of trees in the Białowieża Primeval Forest in 2017, along with subsequent smaller felling in the following years. According to information provided by GreenPeace, about 180,000 trees were cut down during the felling in 2017 [22]. Accurate determination of terrain deforestation is a difficult task without the possibility of field research. However, in the framework of the presented research, such an attempt was made. Analyzes of radiometric indicators were performed to determine changes in the forest cover of the part of the Białowieża Primeval Forest located within the Polish borders. The studies covered the period from 2015 to 2020. The analyzes allowed to detect in which areas in a given year there was a significant change suggesting logging, and in which areas the quality of vegetation improved.

2. VEGETATION INDICES

The vegetative state of plants can be evaluated using multiple indices. The values of these indicators are obtained on the basis of an appropriate combination of values recorded on individual bands. Below there is a sample of 10, described in the literature, indices. Chosen values are commonly used for the assessment of various aspects of vegetation cover.

1. Enhanced Vegetation Index [23]

$$\mathrm{EVI} = 2.5 \times \frac{\mathrm{NIR} - \mathrm{Red}}{\mathrm{NIR} + (6 \times \mathrm{Red}) - (7.5 \times \mathrm{Blue}) + 1}$$

2. Enhanced Normalized Difference Vegetation Index [24]

$$\mathrm{ENDVI} = \frac{(\mathrm{NIR} + \mathrm{Green}) - (2\mathrm{xBlue})}{(\mathrm{NIR} + \mathrm{Green}) + (2\mathrm{xBlue})}$$

3. Green Difference Vegetation Index [25]

$$\mathrm{GDVI} = \mathrm{NIR} - \mathrm{Green}$$

4. Normalized Difference Vegetation Index [26-28]

$$\mathrm{NDVI} = \frac{\mathrm{NIR} - \mathrm{Red}}{\mathrm{NIR} + \mathrm{Red}}$$

5. Green Atmospherically Resistant Index [29]

$$GARI = \frac{NIR - [Green - \gamma(Blue - Red)]}{NIR + [Green - \gamma(Blue - Red)]}$$

6. Green Ratio Vegetation Index [30]

$$\mathrm{GRVI} = \frac{\mathrm{NIR}}{\mathrm{Green}}$$

7. Leaf Area Index [31,32]

$$\mathrm{LAI} = 3.618 \text{ x } \mathrm{EVI} - 0.118$$

8. Renormalized Difference Vegetation Index [33]

$$\mathrm{RDVI} = \frac{\mathrm{NIR} - \mathrm{Red}}{\sqrt{\mathrm{NIR} + \mathrm{Red}}}$$

9. Soil Adjusted Vegetation Index [34, 35]

$$\mathrm{SAVI} = \frac{1.5 \text{ x } (\mathrm{NIR} - \mathrm{Red})}{\mathrm{NIR} + \mathrm{Red} + 0.5}$$

10. MERIS Terrestrial Chlorophyll Index [36, 37]

$$MTCI = \frac{NIR - Red_{edge}}{Red_{edge} - Red}$$

Where Red_{edge} is the B6 band.

In the presented study, two indices were selected to examine the condition of the tree cover and the anomalies of tree felling in the presented research. These include NDVI and ENDVI. These coefficients were selected because, according to the sources, they are best suited for this type of research [38-41].
NDVI is one of the most commonly used indices dedicated for the evaluation of vegetation. The index is normalized so for green areas it varies from 0 to 1. Depending on the day of the year and the climate, the value of this index for the forest should be in the range from 0.5 to 0.9. NDVI is not a physical quantity, but

it is correlated with the physical properties of the vegetation. It is based on the assumption that vegetation absorbs most of the visible light and reflects near-infrared bands. NDVI has applications in forest research, agriculture and ecological research [26 – 28, 42 - 46].

The Enhanced Normalized Difference Vegetation Index (ENDVI) has been developed by LDP LLC Carlstadt. This index uses the sum of the reflection of the NIR and green bands and its relation to the value of the blue band. The use of the blue band results from the increased absorption of this part of the electromagnetic wave spectrum by chlorophyll. This index has been used in many areas, but most often it can be found in agricultural applications [47 - 48].

3. MATERIAL AND METHODS

The study was carried out for the Białowieża Primeval Forest (Figure 1). Part of the forest is the Białowieża National Park, where 57 % of the area is under strict protection and 39% is under active protection so, forest fleeing is there forbidden. However, in the remaining areas, standard forest management can be carried out and there is no additional legal protection. In recent years, this area has been subject to intensive felling. Therefore, the author of this article will try to investigate how the data from Sentinel-2 is useful for detecting and examining such changes.

The period from 2015 was selected because the satellites of the system were launched this year and the previous data from this system is not available. Obtaining good quality observational data for tested area was a problematic task because, at latitudes where the studied area is located, there are frequent clouds. Therefore, despite the high time resolution of the Sentinel-2 satellites, the images often had to be mosaic from several consecutive sections before being subjected to proper analysis. Data for June was collected for each year. The June data shows the time of intensive growth, however, they are collected immediately after or during logging. At the same time, there is a possibility of intense green lower vegetation that can disturb the image of the forest felling.

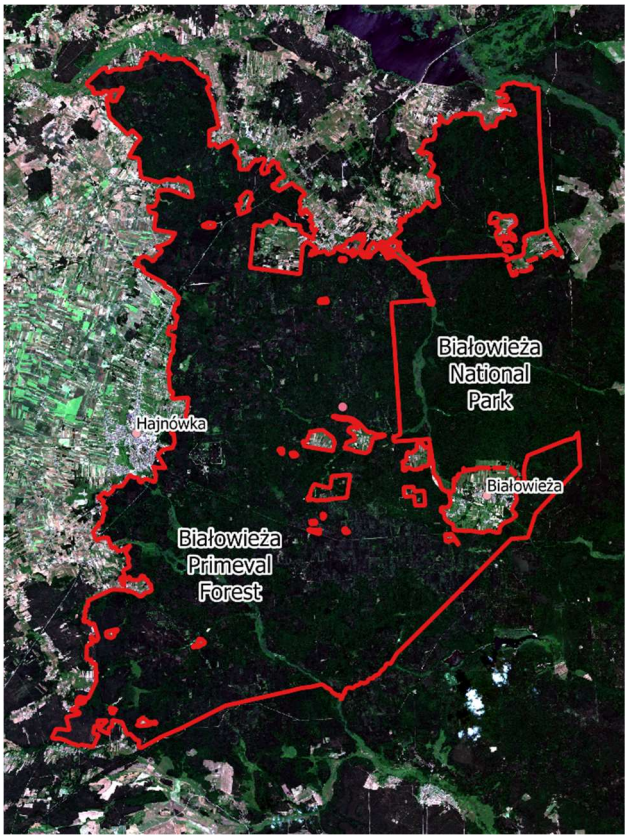

Fig. 1. Białowieża Primeval Forest with Białowieża National Park

The level-1C (top-of-atmosphere reflectance) images were downloaded from the Copernicus server, therefore the atmospheric correction had to be applied to obtain the level-2A sets (bottom-of-atmosphere reflectance). This task was performed using the Sen2Cor [49] script provided by ESA. At the same time images were often cloudy, therefore cloud masking and mosaic had to be done with the use of neighboring satellite images. Usually, it was enough to use the imaging taken from the second satellite of the system (3-days apart). This task was performed using the "Semi-Automatic Classification Plugin" available as a free open source plug in for Qgis software. Then, in "Sentinel image processor" (own software), the bands B2 (Blue), B3 (Green), B4 (Red), and B8 (NIR) were used to calculate the NDVI and ENDVI values. In this way, images with a spatial resolution of 10m were obtained. The resulting images were cropped to the border of the Białowieża Primeval Forest, excluding the Białowieża National Park. Finally, 6 NDVI raster images and 6 ENDVI raster images were obtained (Figure 2).

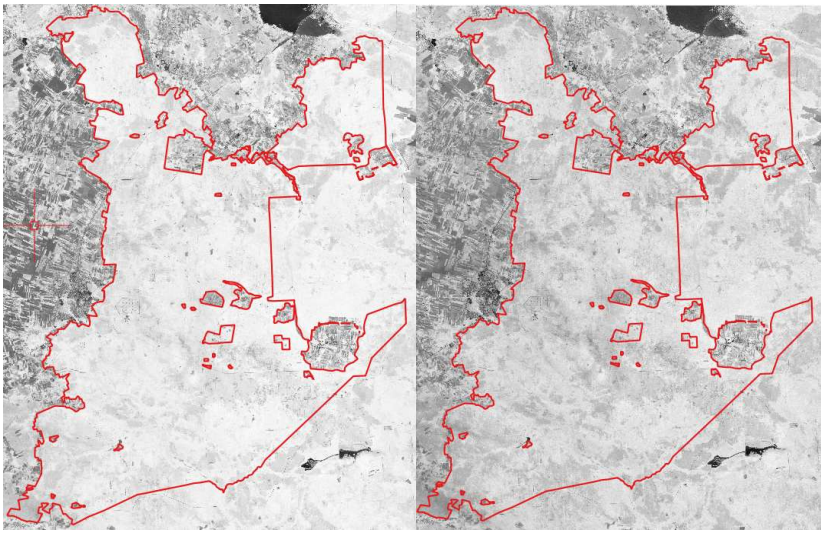

Fig. 2. NDVI raster image (left) and ENDVI raster image (right) examples

The aim of the study was to determine the vegetation state of the forest as well as to detect forest cover anomalies that could be interpreted as forest felling and determine their range for the entire forest area. Therefore, it was necessary to detect anomalies in the values of the NDVI and ENDVI indices for the following years. For this purpose, differentiation of raster images from the appropriate months for successive years was performed. Each obtained differential raster image contained the respective differences in the values of the NDVI or ENDVI coefficients for the successive years (Figure 3). Totally 5 images of NDVI differences and 5 images of ENDVI differences were obtained.

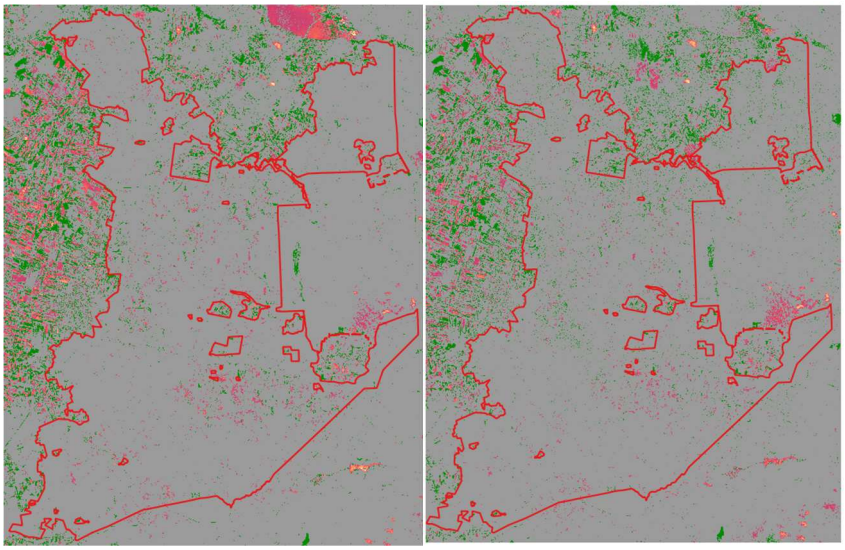

Fig. 3. NDVI differential raster image (left) and ENDVI differential raster image (right) examples

On the obtained images, values close to 0 mean that the quality of vegetation did not change significantly in the following years. Positive values from 0.15 and the highest mean a significant decrease in the quality of vegetation and may be considered areas of deforestation or destruction of the forest cover. In figure 3, values close to 0 (-0.15 to 0.15) are marked in grey, while pink to yellow indicates areas with values above the set threshold value and green is used for negative values below -0.15. The threshold value was established based on known places where forest clearings were performed and the values of NDVI differences that were obtained there. The same applies to the negative values which suggest that the vegetation quality has improved in a given area. However, it should be remembered that this is not synonymous with the regrowth of forest in a given area, but with an increased intensity of green compared to the previous year. This value may be related to the growth rate of lower vegetation in a given year depending on the weather conditions. Then, on the basis of the obtained results, the areas of anomaly for both indexes in the following years were calculated and analyzed. The diagram of the processing steps is shown in Figure 4.

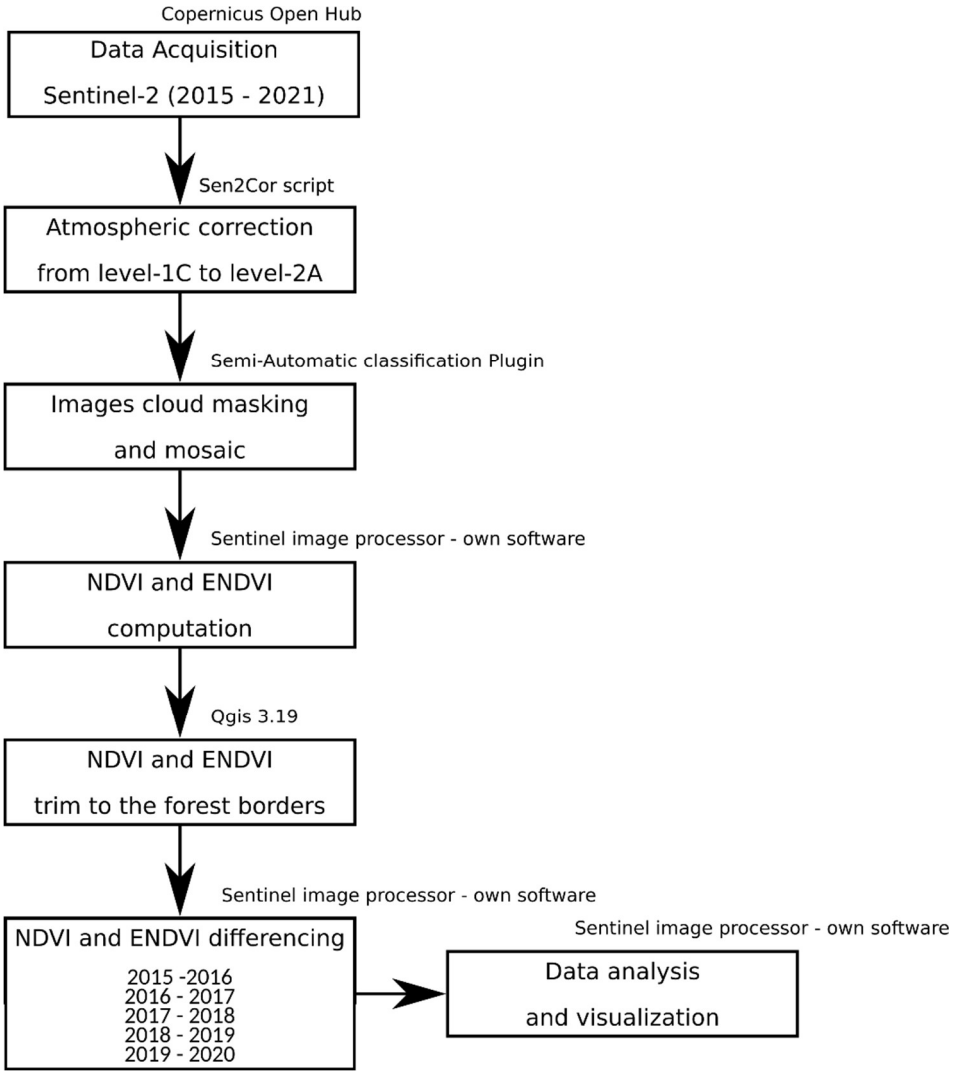

Fig. 4. Sentinel-2 image processing flowchart

4. RESULTS AND DISCUSION

The purpose of the presented study was to assess the suitability of Sentinel-2 data for automatic forest cover changes detection. As mentioned earlier, the NDVI, as well as ENDVI differential raster images from the same seasons for subsequent years of the Sentinel2 mission, were used for this purpose. The study assumes that, on the basis of the detected anomalies in the calculated indices, it is possible to

detect the locations of the cuttings and the places where the quality of the green cover has decreased at the studied area. Below there are pictures of an exemplary area of land where tree felling was carried out during the analyzed period of time (Figure 5 and Figure 6). The left column of Figure 5 shows the images from B2, B3 and B4 bands for subsequent years, while NDVI and ENDVI indices raster images are presented in the middle and right column. The differences in the analyzed indices (NDVI and ENDVI) between consecutive years are in Figure 6.

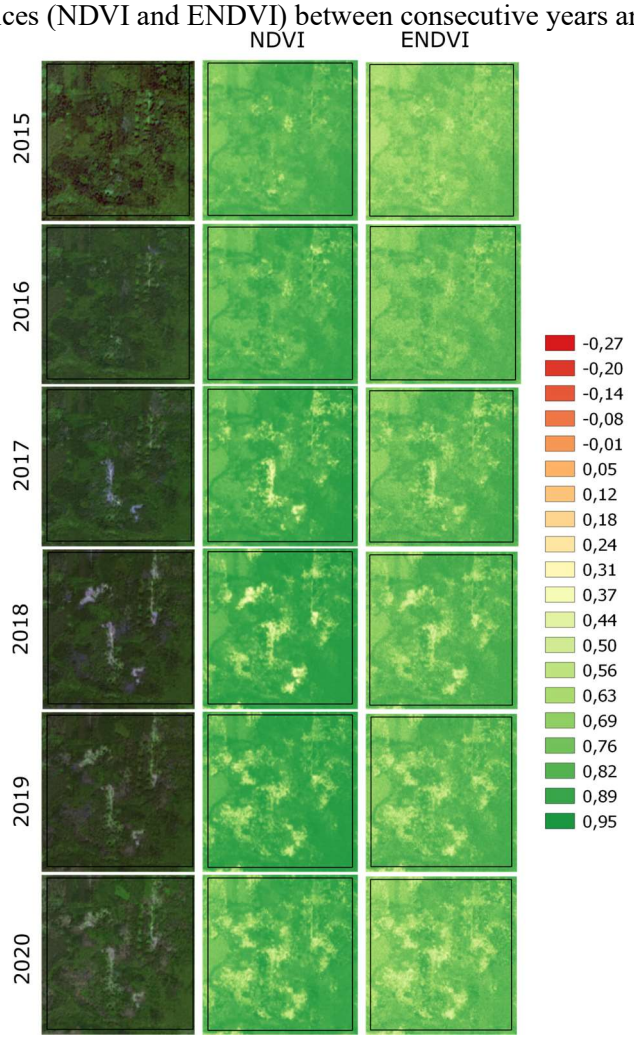

Fig. 5. An example of tree felling visible on subsequent RGB, NDVI and ENDVI raster images

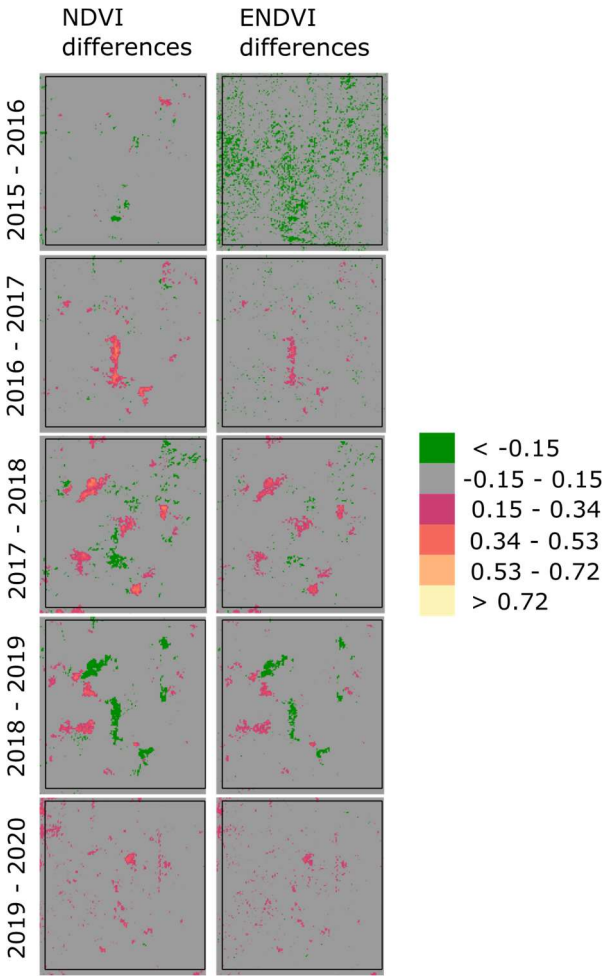

Fig. 6. An example of tree felling visible on subsequent differential raster images

As can be seen in Figures 5 and 6, in the area under consideration, the first logging was carried out between 2016 and 2017, and subsequent logging in subsequent years until 2020. In the forests of the temperate zone, after cutting down tall trees, the process of intensive growth of the undergrowth vegetation begins, and later it is overgrown with a new tree stand, naturally sown or planted. It can be troublesome to clearly distinguish between shrub vegetation or young trees and an old stand on the basis of vegetation indices. Therefore it is appropriate to compare the coefficients in successive years in order to capture the moment of cutting. On the other hand, if the overgrowth was slow or the area was plowed in the meantime, the picture of NDVI and ENDVI anomalies will persist in the

following years (ex. Figure 5, the year 2017 and 2018). That is why, to track changes in the forest cover over the years, it is appropriate to use the differences in vegetation indices between consecutive years. The use of vegetation indices differential raster images allows for automatic detection of forest cover changes that have occurred between subsequent years.

Automatic detection of deforestation on the basis of differential raster images requires limiting the analyzed area strictly to the originally forested area. For this purpose, the Sentinel-2 granules were clipped to the area of Białowieża Primeval Forest. Additionally, built-up areas were excluded from the study, together with the adjacent agricultural areas. The area of non-forested banks of the Leśna River was also problematic. In the case of years 2015 to 2019, the difference between this area and a dense forest, even visible in RGB images, is almost imperceptible in terms of the NDVI or ENDVI indices raster images (Figure 7). In 2021, there is a significant decrease in the value of indices of vegetation for this area, caused by drought, which difference on the differential raster images takes the same values as the tree felling. For this reason, the mentioned area was manually excluded from the study.

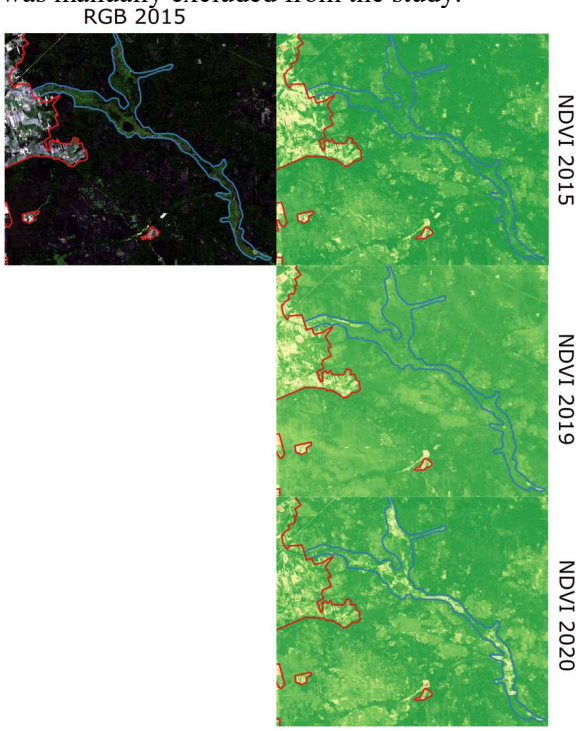

Fig. 7. NDVI anomaly of non-forested banks of the Leśna River

In the conducted research, the NDVI and ENDVI difference raster images were developed for the Białowieża Primeval Forest area (Figures 8 and 9). Some statistics of those differential images have been prepared and presented in Table 2.

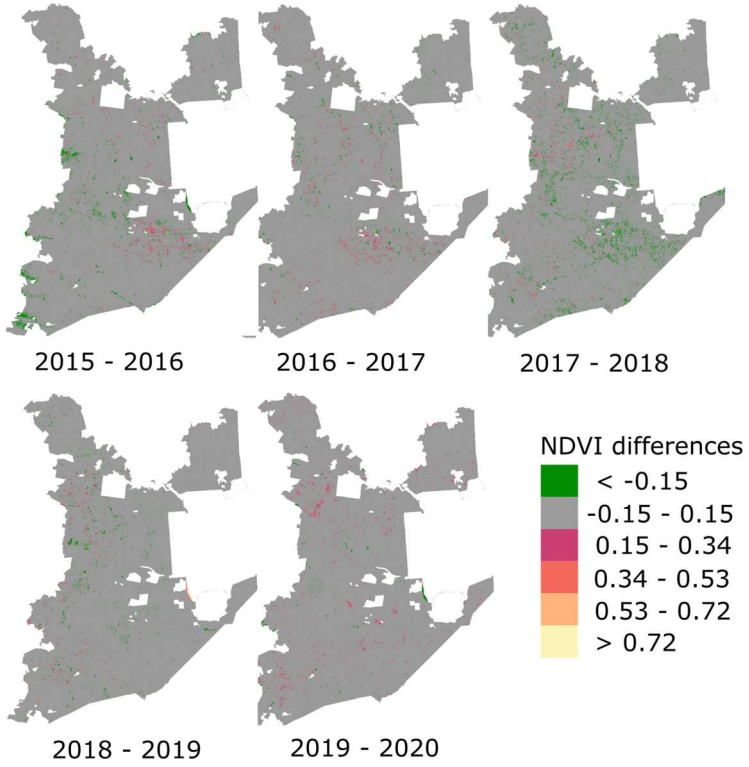

Fig. 8. NDVI differential raster images of Białowieża Primeval Forest

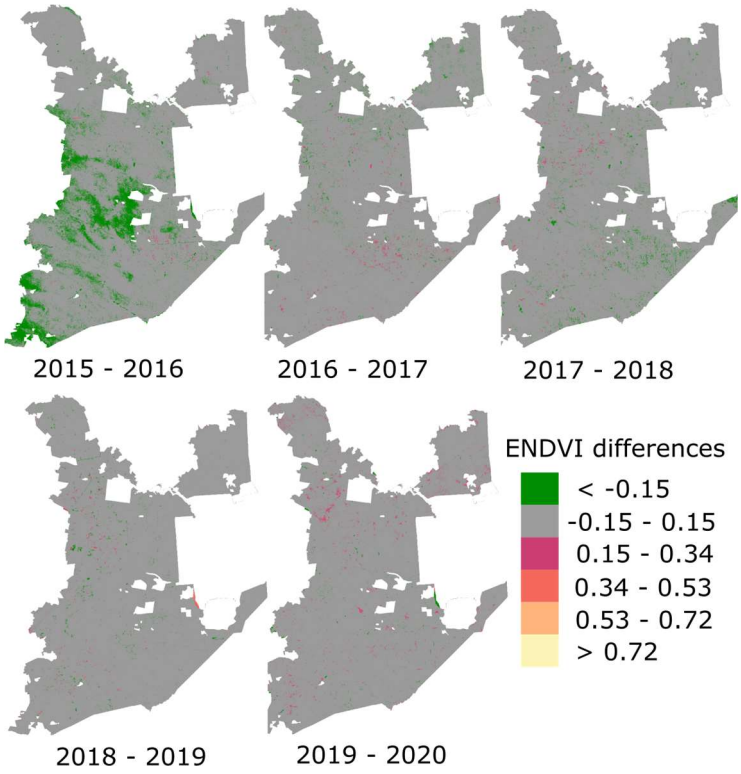

Fig. 9. ENDVI differential raster images of Białowieża Primeval Forest

Based on the analysis of the obtained differential raster images, it can be concluded that the NDVI indicator is better suited for finding logging areas than ENDVI.

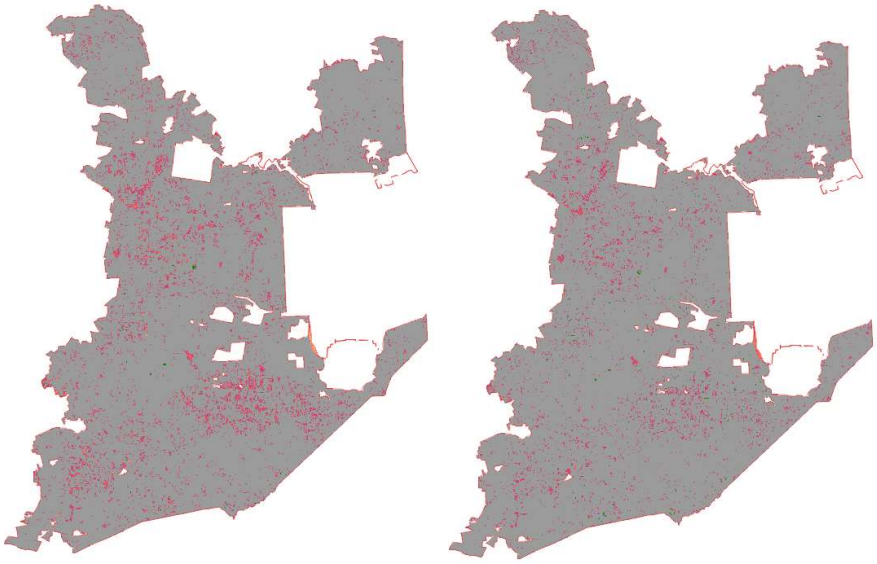

Fig. 10. The summary NDVI (left) and ENDVI (right) raster images

Table 2. Detected logging statistics

Differenced years	Pixels classified as logging	Area [km^2]	Percent of total area
NDVI			
2015 - 2016	51416	5.1416	1.03
2016 - 2017	73139	7.3139	1.46
2017 - 2018	51689	5.1689	1.03
2018 - 2019	43817	4.3817	0.87
2019 - 2020	71624	7.1624	1.43
ENDVI			
2015 - 2016	20169	2.0169	0.40
2016 - 2017	62580	6.2580	1.25
2017 - 2018	48350	4.8350	0.96
2018 - 2019	40255	4.0255	0.80
2019 - 2020	100261	10.0261	2.00

A summary NDVI raster image and a summary ENDVI raster image were used to present the full picture of the tree logging carried out in the analyzed area in the years 2015-2020 (Figure 10). In the raster, the red color is given to pixels which in any year have been qualified as corresponding to the logging.

REFERENCES

1. Gascon, F et al. 2014. Copernicus Sentinel-2 mission: products, algorithms and Cal/Val. Earth observing systems XIX (Vol. 9218, p. 92181E). International Society for Optics and Photonics. https://doi.org/10.1117/12.2062260.
2. Szantoi, Z and Strobl, P 2019. Copernicus Sentinel-2 calibration and validation. European Journal of Remote Sensing, 52:1, 253-255. DOI: 10.1080/22797254.2019.1582840.
3. Drusch, M et al. 2012. Sentinel-2: ESA's optical high-resolution mission for GMES operational services. *Remote sensing of Environment* **120**, 25-36.
4. Addabbo, P, Focareta, M, Marcuccio, S, Votto, C and Ullo, SL 2016. Contribution of Sentinel-2 data for applications in vegetation monitoring. *ACTA IMEKO* **5(2)**, 44-54.
5. Spoto, F et al. 2012. Overview of sentinel-2. *IEEE International Geoscience and Remote Sensing Symposium* 1707-1710.
6. Masek, J, Ju, J, Roger, JC, Skakun, S, Claverie, M and Dungan, J 2018. Harmonized Landsat/Sentinel-2 products for land monitoring. *IGARSS 2018-2018 IEEE International Geoscience and Remote Sensing Symposium* 8163-8165.
7. Zheng, H 2017. Performance evaluation of downscaling Sentinel-2 imagery for land use and land cover classification by spectral-spatial features. *Remote Sensing* **9(12)**, 1274.
8. Abdi, AM 2020. Land cover and land use classification performance of machine learning algorithms in a boreal landscape using Sentinel-2 data. *GIScience & Remote Sensing* **57(1)**, 1-20.
9. Steinhausen, MJ, Wagner, PD, Narasimhan, B and Waske, B 2018. Combining Sentinel-1 and Sentinel-2 data for improved land use and land cover mapping of monsoon regions. *International journal of applied earth observation and geoinformation.* **73**, 595-604.
10. Urban, M 2018. Surface moisture and vegetation cover analysis for drought monitoring in the Southern Kruger National Park using sentinel-1, sentinel-2, and landsat-8. *Remote Sensing* **10(9)**, 1482.
11. Dotzler, S Hill, J Buddenbaum, H and Stoffels, J 2015. The potential of EnMAP and Sentinel-2 data for detecting drought stress phenomena in deciduous forest communities. *Remote Sensing* **7(10)**, 14227-14258.
12. Immitzer, M Vuolo, F and Atzberger, C 2016. First experience with Sentinel-2 data for crop and tree species classifications in central Europe. *Remote sensing* **8(3)**, 166.
13. Erinjery, JJ Singh, M and Kent, R 2018. Mapping and assessment of vegetation types in the tropical rainforests of the Western Ghats using

multispectral Sentinel-2 and SAR Sentinel-1 satellite imagery. *Remote Sensing of Environment* **216**, 345-354.
14. Daryaei, A, Sohrabi, H, Atzberger, C and Immitzer, M 2020. Fine-scale detection of vegetation in semi-arid mountainous areas with focus on riparian landscapes using Sentinel-2 and UAV data. *Computers and Electronics in Agriculture* **177**, 105686.
15. Feng, J, Dong, B, Qin, T, Liu, S, Zhang, J and Gong, X 2021. Temporal and Spatial Variation Characteristics of NDVI and Its Relationship with Environmental Factors in Huangshui River Basin from 2000 to 2018. *Polish Journal of Environmental Studies*.
16. Puletti, N, Chianucci, F and Castaldi, C 2018. Use of Sentinel-2 for forest classification in Mediterranean environments. *Ann. Silvic. Res* **42**, 32-38.
17. Hościło, A and Lewandowska, A 2019. Mapping forest type and tree species on a regional scale using multi-temporal Sentinel-2 data. *Remote Sensing* **11(8)**, 929.
18. Lima, TA, Beuchle, R, Langner, A, Grecchi, RC, Griess, VC and Achard, F 2019. Comparing Sentinel-2 MSI and Landsat 8 OLI imagery for monitoring selective logging in the Brazilian Amazon. *Remote Sensing* **11(8)**, 961.
19. Masiliūnas, D 2017. Evaluating the potential of Sentinel-2 and Landsat Image time series for detecting selective logging in the Amazon. *Wageningen University and Research Centre: Wageningen, The Netherlands*.
20. Khovratovich, T Bartalev, S Kashnitskii, A Balashov, I and Ivanova, A 2020. Forest change detection based on sub-pixel tree cover estimates using Landsat-OLI and Sentinel 2 data. *In IOP Conference Series: Earth and Environmental Science* **507(1)**, 012011.
21. Zhang, Y et al. M. (2021). Tracking small-scale tropical forest disturbances: Fusing the Landsat and Sentinel-2 data record. *Remote Sensing of Environment* **261**, 112470.
22. Pałaś, KW and Zawadzki, J 2020. Sentinel-2 Imagery Processing for Tree Logging Observations on the Białowieża Forest World Heritage Site. *Forests* **11(8)**, 857.
23. Huete, A, Didan, K, Miura, T, Rodriguez, EP, Gao, X and Ferreira, LG 2002. Overview of the radiometric and biophysical performance of the MODIS vegetation indices. *Remote sensing of environment* **83(1-2)**, 195-213.
24. Strong, CJ, Burnside, NG and Llewellyn, D 2017. The potential of small-Unmanned Aircraft Systems for the rapid detection of threatened unimproved grassland communities using an Enhanced Normalized Difference Vegetation Index. *PloS one* **12(10)**, e0186193.
25. Sripada, RP, Heiniger, RW, White, JG and Weisz, R 2005. Aerial color infrared photography for determining late-season nitrogen requirements in corn. *Agronomy Journal* **97(5)**, 1443-1451.

26. Rouse, JW, Haas, RH, Schell, JA and Deering, DW 1974. Monitoring vegetation systems in the Great Plains with ERTS. *NASA special publication* **351(1974)**, 309.
27. Carlson, TN and Ripley, DA 1997. On the relation between NDVI, fractional vegetation cover, and leaf area index. *Remote sensing of Environment* **62(3)**, 241-252.
28. Pettorelli, N, Vik, JO, Mysterud, A, Gaillard, JM, Tucker, CJ and Stenseth, NC 2005. Using the satellite-derived NDVI to assess ecological responses to environmental change. *Trends in ecology & evolution* **20(9)**, 503-510.
29. Gitelson, AA and Merzlyak, MN 1998. Remote sensing of chlorophyll concentration in higher plant leaves. *Advances in Space Research* **22(5)**, 689-692.
30. Ballester, C, Brinkhoff, J, Quayle, WC and Hornbuckle, J 2019. Monitoring the Effects of Water Stress in Cotton Using the Green Red Vegetation Index and Red Edge Ratio. *Remote Sensing* **11(7)**, 873.
31. Price, JC 1993. Estimating leaf area index from satellite data. *IEEE Transactions on Geoscience and Remote Sensing* **31(3)**, 727-734.
32. Chen, JM and Black, TA 1992. Defining leaf area index for non-flat leaves. *Plant, Cell & Environment* **15(4)**, 421-429.
33. Haboudane, D, Miller, JR, Pattey, E, Zarco-Tejada, PJ and Strachan, IB 2004. Hyperspectral vegetation indices and novel algorithms for predicting green LAI of crop canopies: Modeling and validation in the context of precision agriculture. *Remote sensing of environment* **90(3)**, 337-352.
34. Huete, AR 1988. A soil-adjusted vegetation index (SAVI). *Remote sensing of environment* **25(3)**, 295-309.
35. Gilabert, MA, González-Piqueras, J, Garcıa-Haro, FJ and Meliá, J 2002. A generalized soil-adjusted vegetation index. *Remote Sensing of environment* **82(2-3)**, 303-310.
36. Dash, J and Curran, PJ 2007. Evaluation of the MERIS terrestrial chlorophyll index (MTCI). *Advances in Space Research* **39(1)**, 100-104.
37. Dash, J, Jeganathan, C and Atkinson, PM 2010. The use of MERIS Terrestrial Chlorophyll Index to study spatio-temporal variation in vegetation phenology over India. *Remote Sensing of Environment* **114(7)**, 1388-1402.
38. Susantoro, TM, Wikantika, K, Saepuloh, A and Harsolumakso, AH 2018. Selection of vegetation indices for mapping the sugarcane condition around the oil and gas field of North West Java Basin, Indonesia. *In IOP Conference Series: Earth and Environmental Science* **149(1)**, 012001.
39. Lasaponara, R 2006. On the use of principal component analysis (PCA) for evaluating interannual vegetation anomalies from SPOT/VEGETATION NDVI temporal series. *Ecological modelling* **194(4)**, 429-434.

40. Anyamba, A and Tucker, CJ 2005. Analysis of Sahelian vegetation dynamics using NOAA-AVHRR NDVI data from 1981–2003. *Journal of arid environments* **63(3)**, 596-614.
41. Susantoro, TM Wikantika, K Saepuloh, A and Harsolumakso, AH 2018. Utilization of vegetation indices to interpret the possibility of oil and gas microseepages at ground surface. *In IOP Conference Series: Earth and Environmental Science* **145(1)**, 012012.
42. Kumar, P, Rani, M, Pandey, PC, Majumdar, A and Nathawat, MS 2010. Monitoring of deforestation and forest degradation using remote sensing and GIS: A case study of Ranchi in Jharkhand (India). *Report and opinion* **2(4)**, 14-20.
43. Mkhabela, MS, Bullock, P, Raj, S, Wang, S and Yang, Y 2011. Crop yield forecasting on the Canadian Prairies using MODIS NDVI data. *Agricultural and Forest Meteorology* **151(3)**, 385-393.
44. Pettorelli, N 2013. The normalized difference vegetation index. *Oxford University Press*.
45. Sruthi, S and Aslam, MM 2015. Agricultural drought analysis using the NDVI and land surface temperature data; a case study of Raichur district. *Aquatic Procedia* **4**, 1258-1264.
46. Vicente-Serrano, SM, Cuadrat-Prats, JM and Romo, A 2006. Early prediction of crop production using drought indices at different time-scales and remote sensing data: application in the Ebro Valley (north-east Spain). *International Journal of Remote Sensing* **27(3)**, 511-518.
47. Kushida, K et al. 2010. Spectral indices for remote sensing of phytomass and deciduous shrub changes in Alaskan arctic tundra. *In AGU Fall Meeting Abstracts* **2010**, GC43B-0977.
48. Vasudevan, A, Kumar, DA and Bhuvaneswari, NS 2016. Precision farming using unmanned aerial and ground vehicles. *IEEE Technological Innovations in ICT for Agriculture and Rural Development* 146-150.
49. Main-Knorn, M, Pflug, B, Louis, J, Debaecker, V, Müller-Wilm, U and Gascon, F 2017. Sen2Cor for sentinel-2. *Image and Signal Processing for Remote Sensing XXIII* **10427**, 1042704.

Editor received the manuscript: 06.07.2021